

CHAPTER VI

*Exploration of Solvation
Consequence of surface active
Ionic Liquid with Amino Acids in
Aqueous Enironments by
Physicochemical Contrivance*

VI.1.HIGHLIGHTS

- Interactions act of [BMIM][C₈SO₄] and [MOIM]Cl ILs with amino acids in aq. solution are studied.
- Conductivity has been investigated in aq. IL+ AA solution at different temperatures.
- Conductivity and spectroscopic studies reveal the presence of non-covalent interactions.
- Association constants are evaluated from UV-Vis and are further justified by Fluorescence.
- ¹HNMR study confirmed the interactions between selected ILs and amino acids.

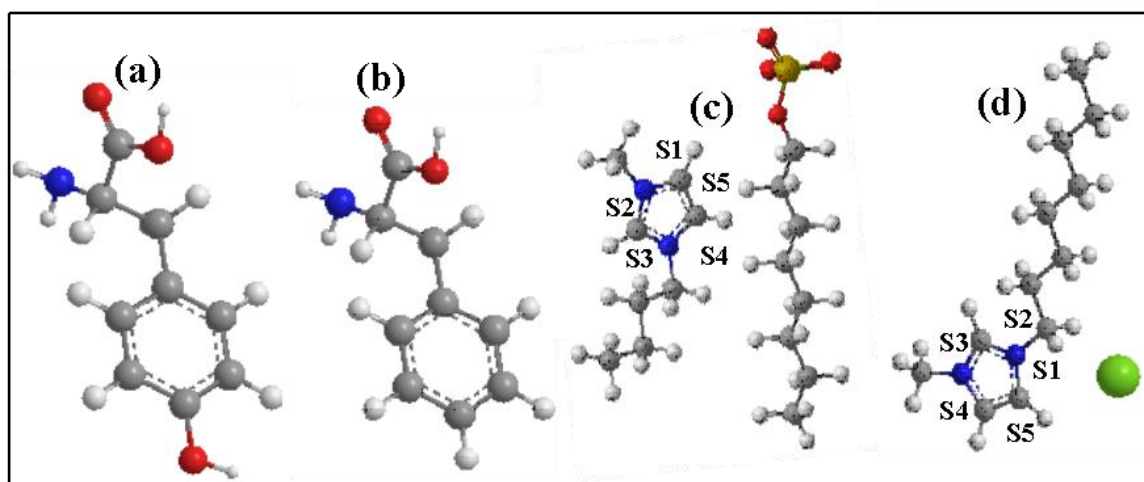
VI.2. INTRODUCTION

Ionic liquids (ILs) belong to the family of those organic compounds which are nano-structured molten salts at room temperature and having cationic organic part and anionic inorganic/organic part [1]. ILs has a spacious diversity of unique physical and chemical character such as non-flammability, negligible vapor pressure, ability of dissolving large variety of compounds, high electrical conductivity etc. [2-6] which makes them a source of interest in different fields of science, industries and process such as biology, separation of amino acids electrochemistry, synthesis etc [7-9]. Additionally they can also be considered as green and designer solvent/electrolytes because of their uniqueness [3, 10-14]. In recent years, ILs are also used to frame the thermophysical properties of aqueous solution containing amino acid(s) (AA) and ILs which provides important information about the intermolecular interactions in solution phase [15-20]. Amino acids are used as model compounds as they are building block of proteins. Such interactions and thermodynamic properties studies helps to overcome the difficulties that arise in case of some biomolecules such as proteins due to their complexed

structures and provides the information about the solute-solvent and solute-solute interactions that can be help to understand the effects of electrolytes on proteins [21-23].

It is already known that 1, 3-disubstituted imidazolium ring based ILs are important enough and widely used in solution chemistry [24-28]. The main significance about the imidazole ring is its existence in various amino acids, proteins and nucleic acids that have many biological activities. Additionally, all protons of 1, 3-disubstituted imidazolium ring are shown acidic character due to delocalization of positive charge over the ring [29].

This work is related to study the molar conductivities (Λ) at three different temperatures (298.15 K, 305.15 K and 312.15 K) and spectroscopic methods (UV-Vis, FTIR) of two amino acids L-tyrosine (L-tyr) and L-phenylalanine (L-Phe) with 1-butyl-3-methylimidazolium octylsulphate [BMIM][C₈SO₄] and 1-methyl-3-octylimidazolium chloride [MOIM]Cl respectively in aqueous solution. All these data have been used to interpret the interactions (non-covalent) involved in ternary (L-tyr/L-Phe + [BMIM][C₈SO₄]/ [BMIM][C₈SO₄] + water) systems. The structure of both AAs and ILs has been shown in **scheme 1**. Moreover, such interactions of analogue imidazolium ILs with L-tyr and L-Phe systems are reported in theoretical background but no such works have been done to propose a model for the studied ILs and amino acids [30].



Scheme.1: Ball & stick representation of (a) L-tyrosine, (b) L-phenylalanine, (c) 1-butyl-3-methylimidazolium octylsulphate [BMIM][C₈SO₄] and (d) 1-methyl-3-octylimidazolium chloride [MOIM]Cl respectively.

VI.3. EXPERIMENTAL SECTION

VI.3.1. Chemicals

The details of chemicals used in this work are listed in **Table 1**; no further purification has been performed. Triply distilled and degassed water (specific conductivity < 1 μ S·cm⁻¹) is used for preparation all solutions.

Table 1: Brief description of the chemicals

SL. No	Name of Chemicals	CAS NO.	Abbreviation	supplier	Purity (mass fraction)
1	1-butyl-3-methylimidazolium octylsulphate	44547-3-58-5	[BMIM][C ₈ SO ₄]	Sigma-Aldrich	≥ 0.95
2	1-methyl-3-octylimidazolium chloride	64697-40-1	[MOIM]Cl	Sigma-Aldrich	≥ 0.97
3	L-tyrosine	60-18-4	L-tyr	Sigma-Aldrich	≥ 0.98
4	L-phenyl alanine	63-91-2	L-phe	Sigma-Aldrich	≥ 0.97

VI.3.2. Apparatus

The mass of chemicals is measured by analytical balance METTLER TOLEDO-Model: AG-285 with an uncertainty ± 0.003 g. All the binary stock solutions are prepared carefully by mass dilution at 298.15 K (± 0.01 K).

The conductance has been carried out in systronic-308 conductivity meter (accuracy ± 0.01) using a dip-type immersion conductivity cell, CD-10, having a cell-constant of $\sim 0.1 \pm 0.001$ cm⁻¹. Experiments are made in thermostatic jacket to maintain temperatures. The specific conductances (κ) of IL+ aq. amino acid solutions under investigation in three different temperatures (298.15 K, 305.15 K, and 312.15 K) are measured. The molar conductance (Λ) for the studied solutions has been calculated using following equation 1 and given in **Figure 1** and **Figure 2**.

$$\Lambda = 1000 \kappa / c \quad (1)$$

Where, c is the molar concentration of amino acids in the studied solution.

UV-visible spectra were recorded by JASCO V-530 UV/VIS Spectrophotometer. All the absorption spectra were recorded at $25^\circ\text{C} \pm 1^\circ\text{C}$.

A photon Technology International (PTI), USA fluorescence spectrophotometer (Quantamaster-40) was used to record fluorescence spectra.

NMR spectra were recorded at 600 MHz Bruker ADVANCE at 298.15K in D₂O. Signals are quoted as δ values in ppm using residual protonated solvent signals as internal standard (D₂O: δ 4.700 ppm). Data are reported as chemical shift.

VI.4. RESULTS AND DISCUSSION

VI.4.1. Conductance study

The conductance study of the interaction (solute-solvent) between the ILs ([BMIM][C₈SO₄]/[MOIM]Cl) with aqueous solution of L-tyr and L-phe amino acids has been performed at three different temperatures. The advantage of this study is that this measurement provides information about the interaction and transport phenomena of the (AA + ILs + water) ternary systems.

The molar conductivities (Λ) of aqueous [BMIM][C₈SO₄] and [MOIM]Cl has been monitored with increasing the concentration of L-tyr and L-phe respectively at three different temperatures and have been listed in **Table 2** and **Table 3**. The **Figure 1** and **Figure 2** show the resulting plots of ([BMIM][C₈SO₄] + L-tyr + water) (system 1), ([MOIM]Cl + L-tyr + water) (system 2), ([BMIM][C₈SO₄] + L-phe + water) (system 3) and ([MOIM]Cl + L-phe + water) (system 4) respectively. For each system it has been observed that Λ values increase with increase in temperature and gradual addition of AA to ILs solution causes a continuous decrease in molar conductance [31-34].

The decrease in molar conductance may be due to two factors- (i) involvement in non-covalent interactions of ILs with AA(s) [20,32,34] and (ii) [BMIM][C₈SO₄] and [MOIM]Cl is an anionic and cationic surface active ionic liquid (SAILs) respectively [35]. So, they have a positive tendency to form micelles after a certain concentration. Initially as there are no micelles, the free mobile ions of SAILs are accountable for the speedy decrease in Λ values with increasing amino acids content in solutions because of increasing system viscosity as well as the attractions between ILs and AAs with increasing AAs concentration. The strong intermolecular hydrophobic-hydrophobic attraction, and other non-covalent (vander Walls, hydrophilic, $\pi \cdots \pi$ interactions, columbic attraction etc.) interactions must have been developed with amino acids [36] but after a certain point the ions contribution are less in transport change and leading to

level off. As the [BMIM][C₈SO₄] SAIL has to some extent more acidic protons and less hindered imidazolium ring protons [30] and long hydrophobic alkyl chain in counter ion part than the [MOIM]Cl, so the former IL must be involved in good interactions than [MOIM]Cl with the amino acids. Apart from these interactions, L-tyr has an extra hydroxyl (-OH) group at para position which helps to bind the ILs more firmly by H-bond than L-phe and involved in strong interactions with the ILs than L-phe. Thus considering all of these the stability order of interactions follows the order of- (system 1)> (system 2)> (system 3)> (system 4).

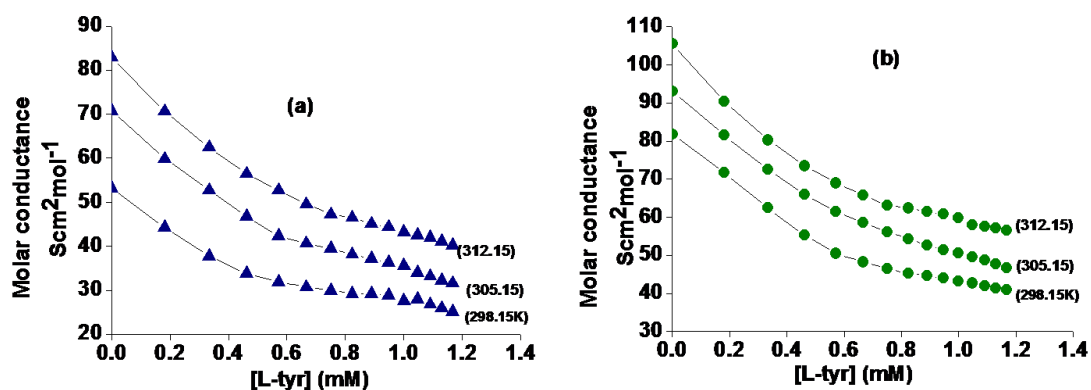


Figure 1. Molar conductivity of (a) [BMIM][C₈SO₄] in aqueous solution with L-tyr and (b) [MOIM]Cl in aqueous solution with L-tyr at three different temperatures.

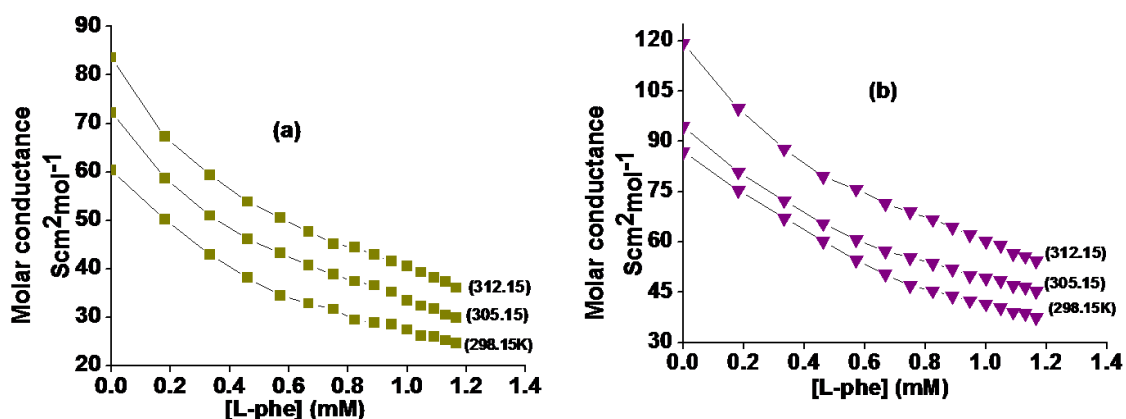


Figure 2. Molar conductivity of (a) [BMIM][C₈SO₄] in aqueous solution with L-phe and (b) [MOIM]Cl in aqueous solution with L-phe at three different temperatures.

Table 2: Conductivity values for the [BMIM][C₈SO₄] and [MOIM]Cl IL with L-tyr in aqueous at three different temperatures(K^a).

Total vol. (mL)	Conc. of L-tyr (mM)	Molar conductance (S cm ² mol ⁻¹) of [BMIM][C ₈ SO ₄]			Molar conductance (S cm ² mol ⁻¹) of [MOIM]Cl		
		298.15 K	305.15	312.15	298.15 K	305.15	312.15
10	0.0	53.14	70.72	82.92	86.93	93.40	119.51
11	0.1818	44.28	59.85	70.66	71.64	81.53	90.36
12	0.3333	37.74	52.76	62.54	62.47	72.55	80.24
13	0.4615	33.83	46.77	56.47	55.25	66.23	73.45
14	0.5714	31.91	42.32	52.72	50.48	61.41	68.93
15	0.6667	30.78	40.67	49.58	48.20	58.56	65.84
16	0.75	29.93	39.53	47.25	46.41	56.22	63.11
17	0.8235	29.26	38.17	46.51	45.23	54.37	62.38
18	0.8889	29.18	37.22	45.11	44.66	52.64	61.46
19	0.9474	28.89	36.31	44.4	43.94	51.45	60.79
20	1.0	27.59	35.62	43.26	43.17	50.62	59.74
21	1.0476	27.19	34.03	42.54	42.65	49.51	58.01
22	1.0909	26.84	33.21	41.97	41.90	48.84	57.53
23	1.13	25.98	32.24	41.14	41.40	48.16	57.08
24	1.1667	25.32	31.67	40.25	40.93	47.61	56.53

^a Standard uncertainties in temperature (T)=0.01.

Table 3: Conductivity values for the [BMIM][C₈SO₄] and [MOIM]Cl IL with L-phe in aqueous at three different temperatures(K^a).

Total vol. (mL)	Conc. of L-tyr (mM)	Molar conductance (S cm ² mol ⁻¹) of [BMIM][C ₈ SO ₄]			Molar conductance (S cm ² mol ⁻¹) of [MOIM]Cl		
		298.15 K	305.15 K	312.15 K	298.15 K	305.15 K	312.15 K
10	0.0	60.35	72.27	83.62	86.92	93.55	119.34
11	0.1818	50.26	58.68	67.26	75.43	80.89	99.86
12	0.3333	42.84	50.95	59.37	67.15	72.35	87.72

13	0.4615	38.19	46.15	53.82	60.27	65.51	79.59
14	0.5714	34.45	43.25	50.55	54.59	60.68	75.74
15	0.6667	32.85	40.74	47.65	50.36	57.34	71.45
16	0.75	31.65	38.77	45.16	46.92	55.32	68.96
17	0.8235	29.45	37.41	44.46	45.45	53.56	66.75
18	0.8889	28.91	36.53	42.86	43.78	51.88	64.34
19	0.9474	28.53	35.22	41.57	42.53	50.02	62.23
20	1.0	27.42	33.49	40.53	41.47	49.19	60.15
21	1.0476	26.09	32.31	39.25	40.39	48.45	59.04
22	1.0909	25.94	31.72	38.17	39.04	47.06	58.19
23	1.13	25.01	30.45	37.32	38.71	46.53	57.41
24	1.1667	24.62	29.91	36.05	37.47	45.25	56.95

^a Standard uncertainties in temperature (T)=0.01K

VI.4.2. UV-vis spectroscopy

The UV-vis spectroscopy is a suitable method that not only helps to get the important information about interaction behavior in systems but also provide the binding nature of binding partners [37]. The absorption peak of [BMIM][C₈SO₄] and [MOIM]Cl in aqueous solution by varying concentration of amino acids (i.e. L-tyr and L-phe) are shown in figure 3 and figure 4 . The strong absorption peaks for both two imidazolium based ILs appeared at ~210 nm (λ_{\max}) [38]. From **Figure 3** and **Figure 4**, it is seen that continuous increase in absorption intensity has been occurred due to regular addition of different concentrated amino acids to both the ILs. Such spectral shifts due to the occurrence of $\pi \cdots \pi$ and C-H \cdots π interactions that may involved in the ILs and L-tyr and L-phe.

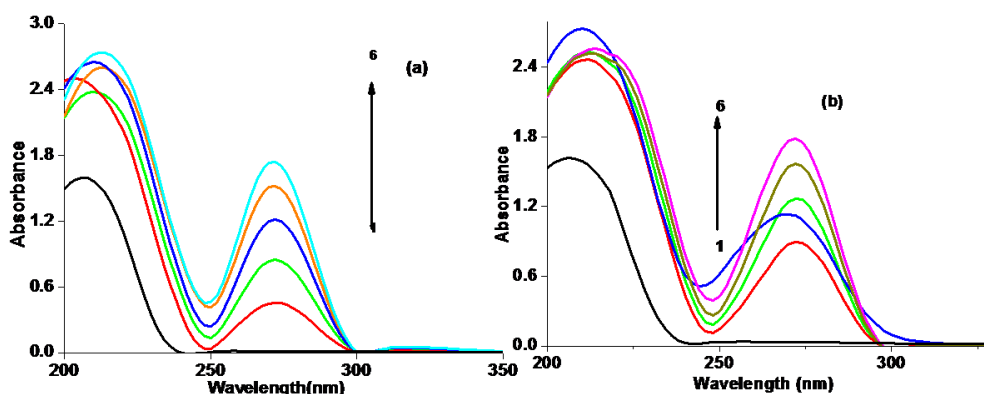


Figure 3. Adsorption spectra of (a) [BMIM][C₈SO₄] and (b) [MOIM]Cl at different concentration of L-tyrosine (1) absence of L-tyrosine, (2) 0.0004 M, (3) 0.0008 M, (4) 0.0012 M, (5) 0.0016 M, (6) 0.0018 M, (7) 0.002 M respectively.

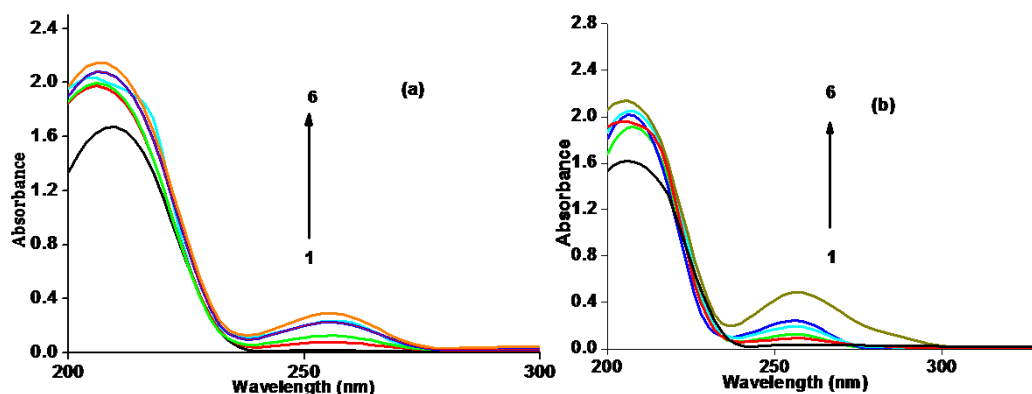


Figure 4. Adsorption spectra of (a) [BMIM][C₈SO₄] and (b) [MOIM]Cl at different concentration of L-phenylalanine (1) absence of L-phenylalanine, (2) 0.0004 M, (3) 0.0008 M, (4) 0.0012 M, (5) 0.0016 M, (6) 0.0018 M, (7) 0.002 M respectively.

VI.4.3. Steady state fluorescence Study

The interactions phenomena of the imidazolium ILs with the amino acids have further been further investigated by fluorescence technique [39]. The imidazolium ring of the ILs is responsible for giving significant emission spectra in fluorescence. The emission peak of both ILs are close enough to each other and appeared at $\sim\lambda_{\text{flu_max}}^{\text{flu}}$ 420 nm when excited by light at wavelength 210 nm [40]. This also implies the less contribution of alkyl chain of [BMIM][C₈SO₄] and [MOIM]Cl imidazolium

based ILs in emission spectra. By keeping constant concentration of ILs in aqueous solution and gradually addition of increase in concentration of amino acids causing the continuous enhancement of the fluorescence intensities of both ILs which indicate that molecular interactions/associations are obviously arising there (Figure 5 and Figure 6).

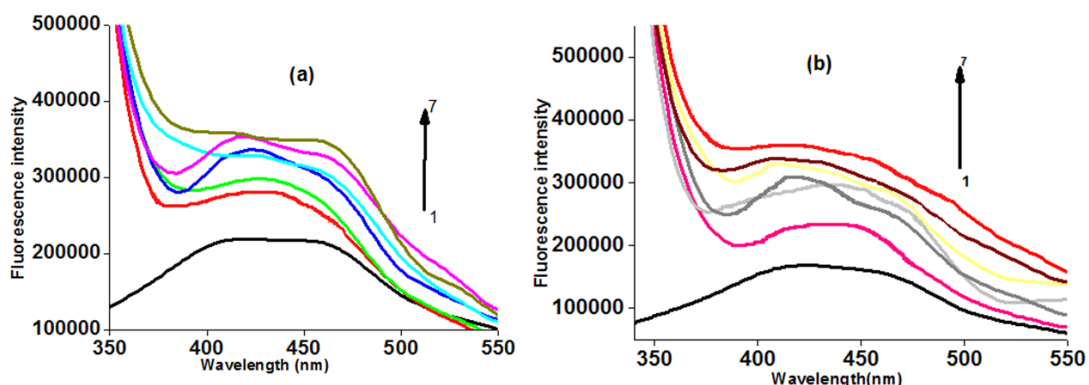


Figure 5. Fluorescence spectra of (a) [BMIM][C₈SO₄] and (b) [MOIM]Cl at different concentration of L-tyrosine (1) absence of L-tyrosine, (2) 0.0003 M, (3) 0.0006 M, (4) 0.0009 M, (5) 0.0012 M, (6) 0.0015 M, (7)0.0018 M respectively.

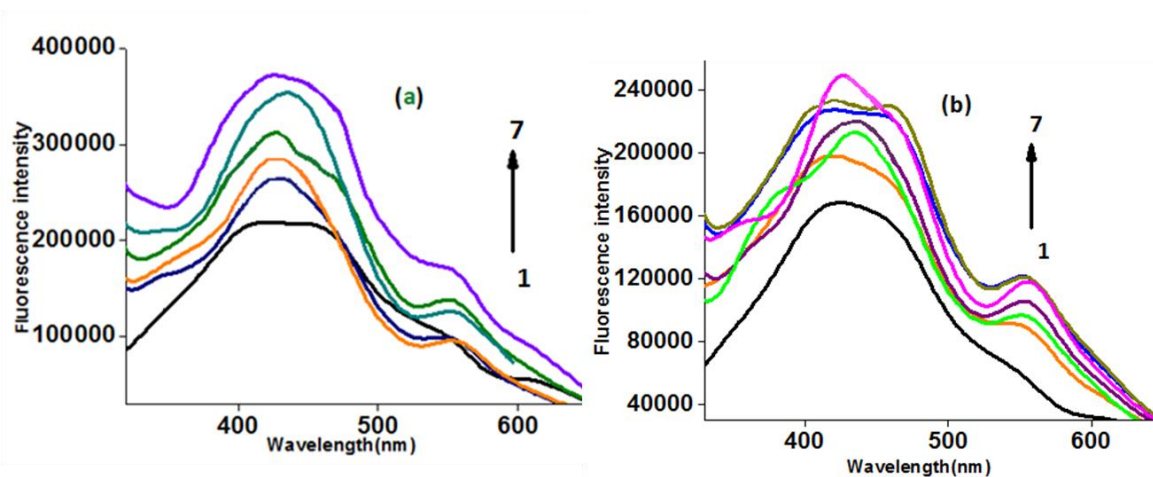


Figure 6. Fluorescence spectra of (a) [BMIM][C₈SO₄] and (b) [MOIM]Cl at different concentration of L-phenylalanine (1) absence of L-phenylalanine, (2) 0.0003 M, (3) 0.0006 M, (4) 0.0009 M, (5) 0.0012 M, (6) 0.0015 M, (7)0.0018 M respectively.

VI.4.4. Determination of association constant-spontaneity and features of interactions

The association constant in this phenomena i.e. [BMIM][C₈SO₄] / [MOIM]Cl ILs interactions with L-tyr and L-phe have been calculated by Benesi-Hildebrand equation 2 [37,38,41] using the absorption and emission spectral (fluorescence) data (**Table 4** and **Table 7**). This is very helpful method for quantitative estimation of extent of binding of two binding events.

$$\frac{1}{I-I_0} = \frac{1}{K_a(I_1-I_0)} \cdot \frac{1}{[AA]} + \frac{1}{(I_1-I_0)} \quad (2)$$

Where, I_0 and I are the intensity values of absorption/ fluorescence of both IL in absence and presence of AAs respectively. I_1 is the intensity of absorption/ fluorescence of ILs due to association with amino acids and K_a is the association constant.

The double reciprocal plots of $1/I-I_0$ versus $1/[AA]$ for all the systems have been shown in **Figure 7** and **Figure 8** and all system are within good linear correlation ($R^2 > 0.900$) and suggest the 1:1 interaction is present for each systems. The K_a values have been calculated from the ratio of intercept and slop of each plot. It can be observed from the K_a value that the association for [BMIM][CSO₄] is greater with L-tyr than L-phe and least for ([MOIM]Cl +L-phe) system.

Further by using the value of K_a the free energy changes (ΔG) for the adduct formation of ILs and AAs have been calculated using the following the equation 3

$$\Delta G = -RT \ln K \quad (3)$$

The values of ΔG for all adducts have been listed in **Table 4** to **Table 7** and the negative values be a sign of the feasibility of the adducts formation by interactions.

The values of K_a and ΔG make known that (system 1) have greater attraction possibility than the others. In theoretically background, the possibility of such an interaction on for an analogue system is reported earlier [30]. Thus, we can endorsed that a stronger H-bond and $\pi \cdots \pi$ stacking interactions are developed in case of L-tyr than L-phe from S2 side (**scheme 1**) that can enhance the stability and can also be attributed for such order of interactions. Further the weak columbic force of attraction between the positively charged ring cation and the negatively charged AA plays a role in bringing them close to each other.

Table 4: Data for the Benesi-Hildebrand double reciprocal plot obtained from UV-Vis spectroscopy for aqueous [BMIM][C₈SO₄] and [MOIM]Cl ILs with L-tyr system at 298.15K^a.

[BMIM][C ₈ SO ₄] (M)	Conc. of L-tyr (M)	I ₀	Intensity (I)	K _a (M ⁻¹)	ΔG KJ mol ⁻¹
4 x 10 ⁻⁴	0.0004		2.43106		
	0.0008		2.53914		
	0.0012	1.61436	2.56891	9260	-22.64
	0.0016		2.60076		
	0.002		2.65974		
[MOIM]Cl (M)	Conc. of L-tyr (M)	I ₀	Intensity (I)	K _a (M ⁻¹)	ΔG KJ mol ⁻¹
4 x 10 ⁻⁴	0.0004		2.31916		
	0.0008		2.44828		
	0.0012	1.67759	2.50968	4994	-21.11
	0.0016		2.54860		
	0.002		2.59924		

^a Standard uncertainties in temperature (T)=0.01K.

Table 5: Data for the Benesi-Hildebrand double reciprocal plot obtained from UV-Vis spectroscopy for aqueous [BMIM][C₈SO₄] and [MOIM]Cl ILs with L-phe system at 298.15K^a.

[BMIM][C ₈ SO ₄] (M)	Conc. of L- phe (M)	I ₀	Intensity (I)	K _a (M ⁻¹)	ΔG KJ mol ⁻¹
4 x 10 ⁻⁴	0.0004		3.45837		
	0.0008		2.60077		
	0.0012	1.61436	2.30684	2373.86	-19.27
	0.0016		2.14971		
	0.002		1.94121		
[MOIM]Cl (M)	Conc. of L- phe (M)	I ₀	Intensity (I)	K _a (M ⁻¹)	ΔG KJ mol ⁻¹
4 x 10 ⁻⁴	0.0004		4.14765		
	0.0008		3.11910		
	0.0012		2.69882		
	0.0016	1.67759	2.49336		-18.98
	0.002		2.25789	2111.78	

^a Standard uncertainties in temperature (T)=0.01K.

Table 6: Data for the Benesi-Hildebrand double reciprocal plot obtained from fluorescence spectroscopy for aqueous [BMIM][C₈SO₄] and [MOIM]Cl ILs with L-tyr system at 298.15K^a.

[BMIM][C ₈ SO ₄] (M)	Conc. of L- tyr (M)	I ₀	Intensity (I)	K _a (M ⁻¹)	ΔG KJ mol ⁻¹
10 x 10 ⁻⁴	0.0003		270750.420		
	0.0006		299469.176		
	0.0009	202353.032	325637.411	1595.67	-18.28
	0.0012		339150.187		
	0.0015		353260.785		
	0.0018		360658.554		
[MOIM]Cl (M)	Conc. of L- tyr (M)	I ₀	Intensity (I)	K _a (M ⁻¹)	ΔG KJ mol ⁻¹

	0.0003		233021.208		
	0.0006		277888.743		
10×10^{-4}	0.0009	158736.743	302731.526	1164.67	-17.50
	0.0012		321062.647		
	0.0015		341268.303		
	0.0018		360191.789		

^a Standard uncertainties in temperature (T)=0.01K

Table 7: Data for the Benesi-Hildebrand double reciprocal plot obtained from fluorescence spectroscopy for aqueous [BMIM][C₈SO₄] and [MOIM]Cl ILs with L-phe system at 298.15K^a.

[BMIM][C ₈ SO ₄] (M)	Conc. of L- phe (M)	I ₀	Intensity (I)	K _a (M ⁻¹)	ΔG KJ mol ⁻¹
	0.0003		257998.969		
	0.0006		279539.343		
10×10^{-4}	0.0009	202353.032	309878.657	1080.00	-17.32
	0.0012		338953.274		
	0.0015		351113.756		
	0.0018		373406.046		
[MOIM]Cl (M)	Conc. of L- phe (M)	I ₀	Intensity (I)	K _a (M ⁻¹)	ΔG KJ mol ⁻¹
	0.0003		190069.494		
	0.0006		213359.573		
10×10^{-4}	0.0009	158736.743	224236.230	933.14	-16.95
	0.0012		236632.444		
	0.0015		237774.593		
	0.0018		249594.135		

^a Standard uncertainties in temperature (T)=0.01.

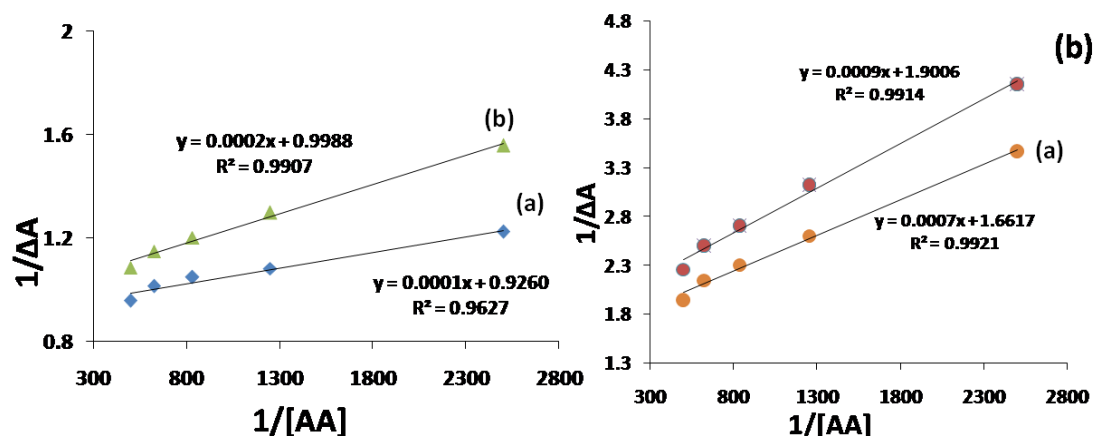


Figure 7. Benesi-Hildebrand plot of $1/\Delta A$ vs. $1/[AA]$ in UV-vis spectroscopy for (a) [BMIM][C₈SO₄] and (b) MOIM]Cl in L-tyr and for (c)[BMIM][C₈SO₄] and (d) MOIM]Cl in L-phe at 298.15K^a.

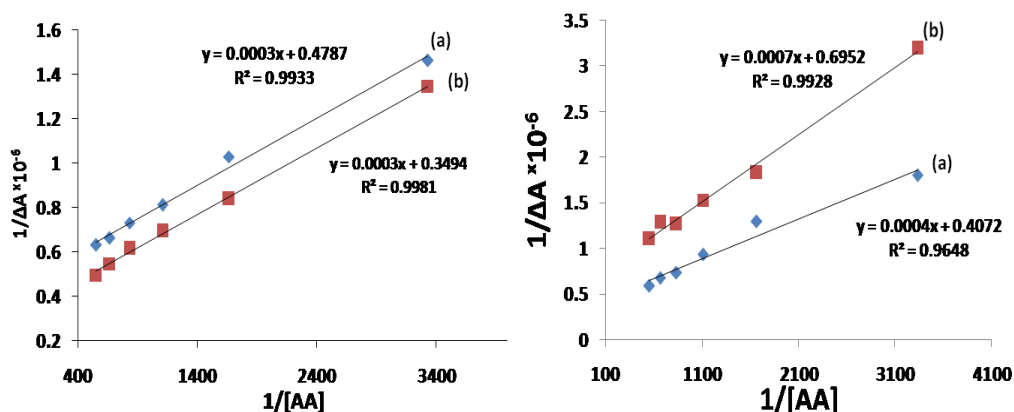


Figure 8. Benesi-Hildebrand plot of $1/\Delta A$ vs. $1/[AA]$ in fluorescence spectroscopy for (a) [BMIM][C₈SO₄] and (b) MOIM]Cl in L-tyr and for (c)[BMIM][C₈SO₄] and (d) MOIM]Cl in L-phe at 298.15K^a.

VI.4.4. NMR Study

Nuclear magnetic resonance (NMR) is a very effectual technique for studying the changes the electronic environment around the different protons of ILs in presence of various kinds of amino acids [41]. In ¹HNMR the binary mixture of

[BMIM][C₈SO₄] and [MOIM]Cl with individual L-tyr and L-phe have been recorded in D₂O at 298.15 K respectively (**Table 8**).

The chemical shifts of [BMIM][C₈SO₄]/ [MOIM]Cl depends on the electronic space environment present in their surrounding area. It is found that significant upfield shifts for alkyl protons of the imidazolium ring have been occurred after mixing of amino acids. This indicates the presence of intermolecular hydrophobic- hydrophobic interactions that leading to increase the electron density around the imidazolium ring. It can be seen from chemical shifts that in both ILs the alkyl chain protons attached to imidazolium ring are in good intermolecular interactions with amino acids but comparing the protons of imidazolium ring, downfield shift for C₂ proton and upfield shifts for other imidazolium ring protons (C₃, C₄) has been observed (**Figure 9, Figure 10**). It most probably suggests the orientation for imidazolium ring that allows strong H-bond formation with C₂ proton and weak $\pi\cdots\pi$ interactions involving C₃, C₄ and benzen ring of AA(s). Thus two opposing influences i.e. H-bond and $\pi\cdots\pi$ interactions are possibly responsible for distinct shifts for ring protons [42]. The downfield shift for C₂ proton of [BMIM] cation is larger than the [MOIM] cation C₂ protons, thus it has been concluded that ([BMIM] cation \cdots AA) H-bonding are somewhat stronger than ([MOIM] cation \cdots AA) interactions. Thus all the variations in chemical shifts are perhaps due to contribution of various factors: such as- (i) H-bond interactions between the acidic proton of ring with oxygen atom of amino acids [(C-H)_{Imidazolium ring} \cdots O_{AA}], (ii) aromatic ring current effect: the $\pi\cdots\pi$ interactions of imidazolium ring with the phenyl ring of amino acid , (iii) weak C-H \cdots π between the cation and AA , (iv) hydrophobic interactions, (v) columbic force of attraction are being there [43, 44] (**Scheme 2**) which are in good agreement with that obtained by our other experiments.

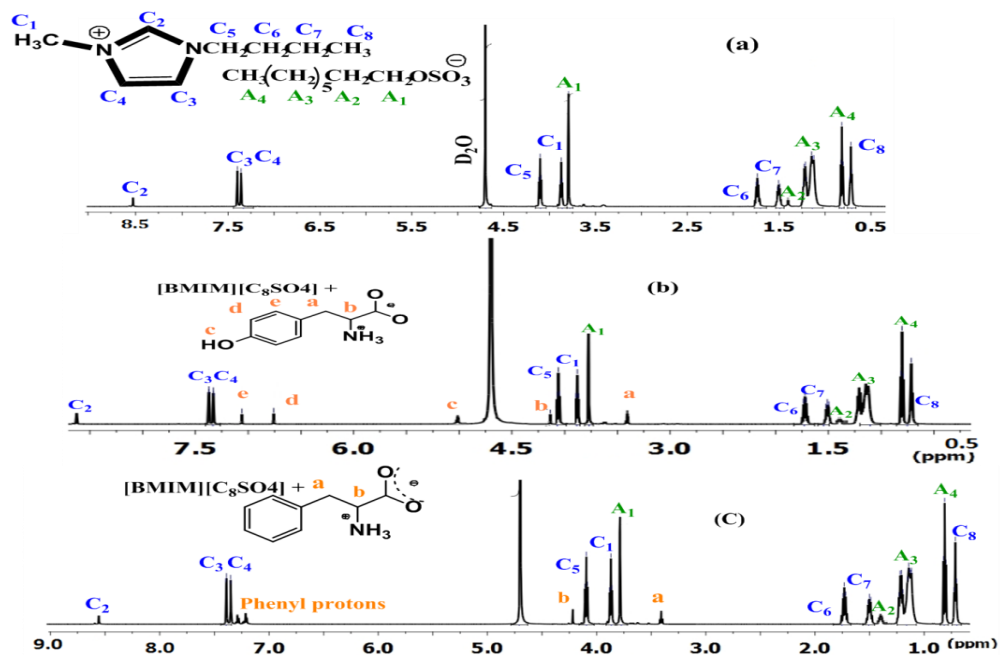


Figure 9. ^1H NMR spectra of (a) $[\text{BMIM}][\text{C}_8\text{SO}_4]$, (b) $([\text{BMIM}][\text{C}_8\text{SO}_4] + \text{L-tyr})$ system and (c) $([\text{BMIM}][\text{C}_8\text{SO}_4] + \text{L-phe})$ system in D_2O at 298.15K.

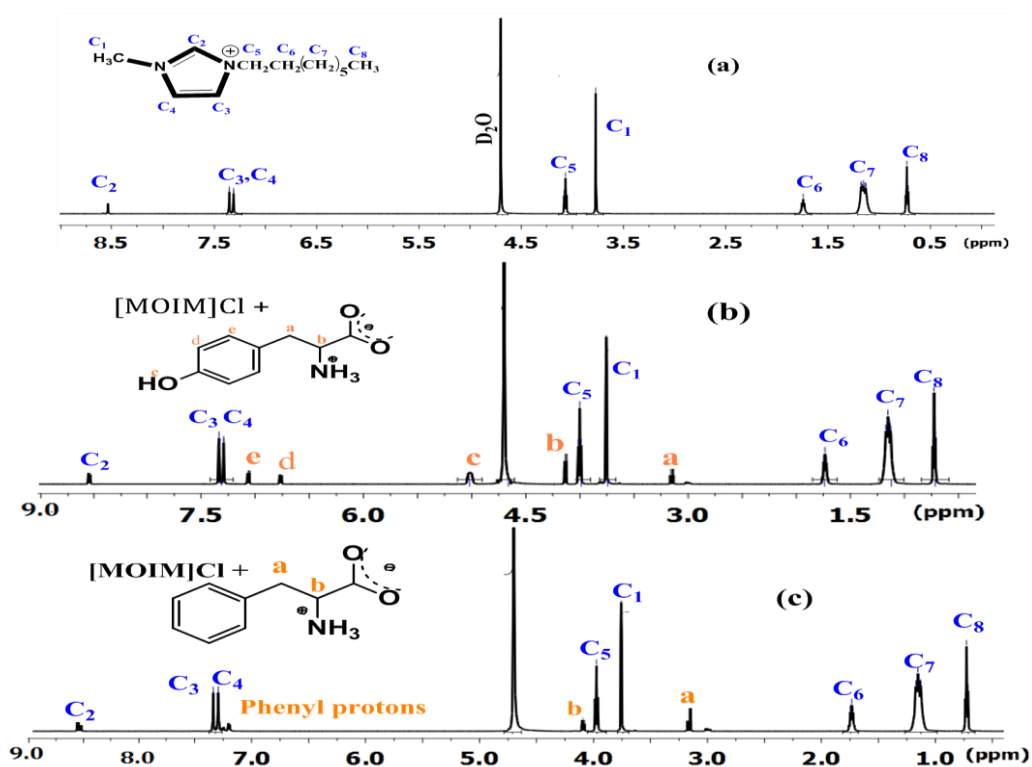
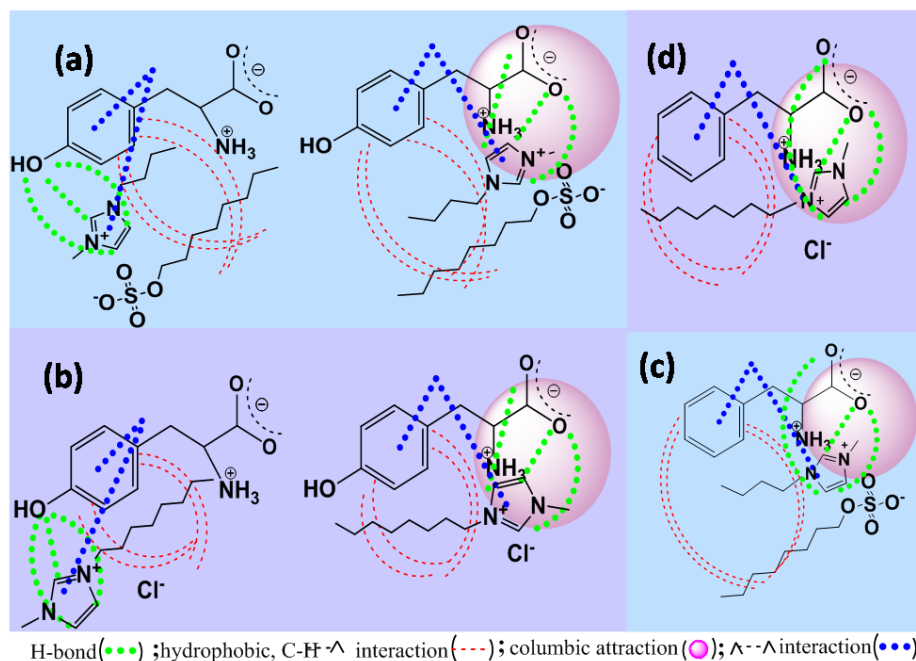


Figure 10. ^1H NMR spectra of (a) $[\text{MOIM}]\text{Cl}$, (b) $([\text{MOIM}]\text{Cl} + \text{L-tyr})$ system and (c) $([\text{MOIM}]\text{Cl} + \text{L-phe})$ system in D_2O at 298.15K.



Scheme 2: Schematic representation of interactions between (a) ([BMIM][C₈SO₄] + L-tyr) (b) ([MOIM]Cl + L-tyr) (c) ([BMIM][C₈SO₄] + L-phe) and (d) ([MOIM]Cl + L-phe) systems in aqueous solution respectively.

Table 8: ¹H NMR chemical shift displacements of [BMIM][C₈SO₄] and [MOIM]Cl in interaction with L-tyr and L-phe in D₂O at 298.15 K^a.

IL protons	Free IL δ (ppm)	IL with L-tyr δ (ppm)	IL with L-phe δ (ppm)
[BMIM][C₈SO₄]			
C1	3.892	3.881	3.884
C2	8.589	8.646	8.598
C3, C4	7.358-7.399	7.328-7.374	7.348-7.392
C5	4.091-4.103	4.070-4.082	4.083-4.095
C6	1.726-1.751	1.711-1.736	1.719-1.744
C7	1.486-1.499	1.481-1.495	1.483-1.489

C8	0.710-0.716	0.707-0.711	0.709-0.714
A1	3.794-3.802	3.774-3.798	3.786-3.800
A2	1.376-1.387	1.372-1.381	1.374-1.383
A3	1.123-1.252	1.115-1.243	1.117-1.248
A4	0.818-830	0.790-0.815	0.787-0.812
<hr/>			
[MOIM]Cl			
C1	3.771	3.756	3.757
C2	8.552	8.602	8.590
C3, C4	7.310-7.356	7.290-7.348	7.297-7.353
C5	4.057-4.068	4.043-4.055	4.040-4.056
C6	1.738-1.749	1.723-1.746	1.720-1.748
C7	1.129-1.161	1.127-1.152	1.127-1.153
C8	0.717-0.741	0.712-0.737	0.714-0.740

VI.5. CONCLUSION

The solute-solvent interaction behavior of studied ionic liquid and amino acids in aqueous solution have been determined by conductance measurements at three different temperatures and spectroscopic studies. The ILs and amino acids systems in aqueous solution indicate the non-covalent interactions among them and causing an increase of hydrodynamic radii of ions and a decrease of their ionic mobility, hence we have got the result a decrease in molar conductance. It has been concluded from the association constant values of the selected ILs with AAs obtained by using Uv-vis and fluorescence measurements that among the two ILs, 1-butyl-3-methylimidazolium octylsulphate [BMIM][C₈SO₄] interact more firmly with L-tyrosine than L-phenylalanine and in each

system both IL and AA have been promoted to each due to non-covalent such as strong hydrophobic- hydrophobic, weak $\pi\cdots\pi$, columbic force of attraction, H-bond interactions etc. amongst themselves. The significant chemical shifts of ILs protons in presence of amino acids in ^1H NMR studies also support the results obtained from other spectroscopic and conductance measurements.

VI.6. REFERENCES

References of CHAPTER VI are given in BIBLIOGRAPHY (Page: 233-235).